Monolithic InP-based fast optical switch module for optical networks of the future

Xi Chen[1], James Regan[2], Tim Durrant[2], Yi Shu[3], George Saridis[3], Georgios Zervas[3], Dimitra Simeonidou[3], Valerija Kamchevska[4], Anna M. Fagertun[4], Siyuan Yu[1,2]

[1]Photonics Group, Department of Electrical and Electronic Engineering, University of Bristol
Merchant Venturers' Building, Bristol, BS8 1UB, United Kingdom
[2]Venture Photonics Ltd
Brixham Laboratory, Freshwater Quarry, Brixham, Devon, TQ5 8BA, United Kingdom
james@venturephotonics.com
[3]HPN Group, Department of Electrical and Electronic Engineering, University of Bristol
Merchant Venturers' Building, Bristol, BS8 1UB, United Kingdom
[4]DTU Fotonik, Department of Photonics Engineering, Technical University of Denmark
Building 343, DK-2800Kgs. Lyngby, Denmark

***Abstract*—We summarized the development of Venture Photonics' sub-10 ns fast optical switch which demonstrates low insertion loss, excellent crosstalk level and polarization independent switching performance.**

***Keywords*—optical switching; photonic integration; optical cross point switch (OXS); optical interconnect; data center networks.**

I. INTRODUCTION

The fast optical switch (FOS) is one of the key enabling optical components for optical packet switching (OPS) [1] and optical burst switching [2]. It brings the benefits of bit rate and format transparency which provide greater agility and flexibility to optical networks. The rise of high performance computing and Data Centre Networks (DCNs) in recent years are driving clearer scenarios for the application of FOS, which could enable a high bandwidth, low latency, energy-efficient optical interconnect among the processing cores, servers and racks compared to its electrical counterpart [3, 4].

Supported by the ECFP7 COSIGN project, Venture Photonics (VPs) is working with University of Bristol (UoB) and Technical University of Denmark (DTU) to develop a new-generation high performance optical crosspoint switch (OXS) module based on the active-vertical-coupling (AVC) technology [5, 6]. As shown in Fig. 1, VPs' OXS module is chosen to serve the fast inter/intra-rack communication in the all-optical DCNs architecture proposed by the HPN group of UoB, in which TDM fast optical circuit switching (OCS) and OPS would be realized and demonstrated, and also to work as a fast TDM switch in the multidimensional-switching-based DCNs designed by the DTU Fotonik.

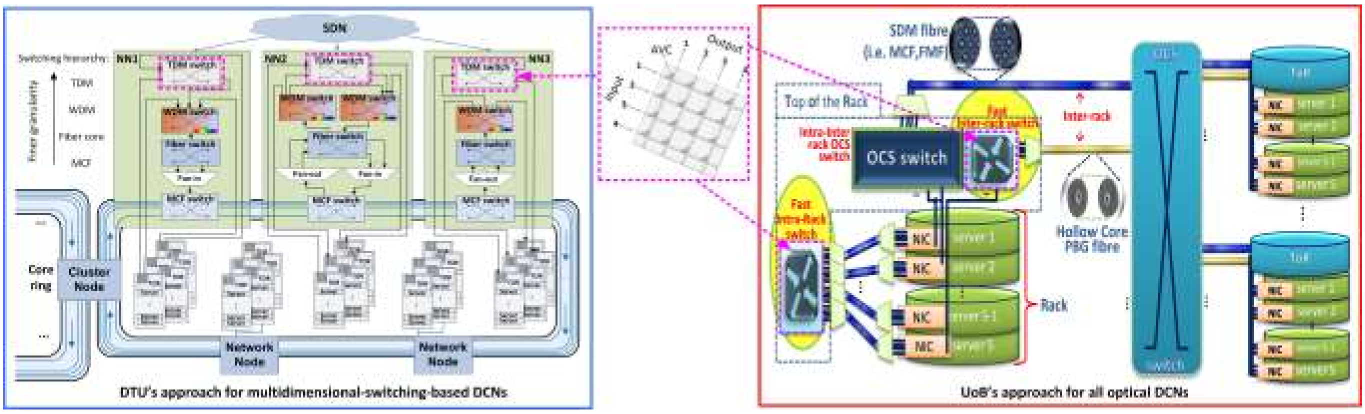

Fig. 1. VPs' 4 × 4 OXS's application in the DCNs architectures proposed by the DTU (left) and UoB (right) respectively
[MCF: Multicore Fiber, NIC: Network Interface Card, ToR: Top of the Rack]

High port-count, compact-size and polarization-independence are highly desirable attributes for a FOS, since the reduction of fiber complexity and the increase of the throughput have always been the main issues facing the designers of the DCNs [7]. In addition, low insertion loss (IL) and negligible crosstalk levels are attractive features to promote signal transmission quality and relax optical power budgets [8]. In this paper we would like to give a review of our 1st generation (Gen-1) AVC-based 4 × 4 OXS device first, which has demonstrated an on-chip lossless sub-10 ns switching as well as an extremely low crosstalk level of <-65 dB for TE mode. A newly-developed Gen-2 OXS model is further introduced, which is assembled in a compact CFP2 form factor with a low-cost packaging technology. The preliminary test results suggests that polarization-independent switching is indeed obtained, paving the way for future commercialization of the high-performance polarization insensitive FOS module.

II. Gen-1 4 × 4 AVC-based OXS and 3-Dimensional Topological Switching Mechanism

The Gen-1 4 × 4 AVC-based OXS device comprises 16 independent switching cells located at the crossing points of the switching grid matrix as depicted in Fig. 1. Fig. 2 gives the individual AVC cell topology and shows how it performs the "On" and "Off" switching. The AVC cell could be divided into three functional regions, which are a lower passive waveguide, sandwiched spacer layer, and upper active waveguide respectively. All the layers in the AVC cell are grown in the InP wafer simultaneously and no regrowth is needed. The effective refractive index of the upper active waveguide (denoted as n_{eff_active}) is designed and tuned to be higher than that of its counterpart (denoted as $n_{eff\_passive}$) to ensure a minimal optical coupling between these two regions under zero bias. Thus the guided lightwave in the passive region will maintain its original propagation through the crossing point, the "Off" state illustrated in Fig. 2(a). On the contrary, Fig. 2(b) shows what the "On" state is like under forward bias. For the AVC cell injected with free carriers, the carrier-induced refractive index change [9] will get the n_{eff_active} decrease

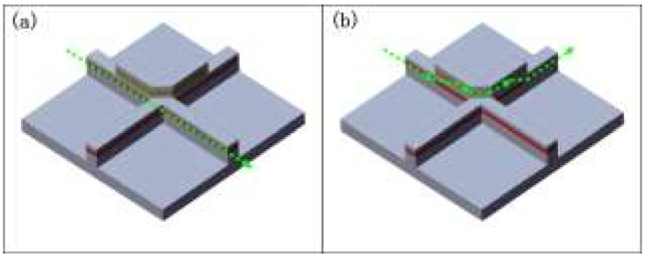

Fig.2. (a): "Off" state under Zero bias and (b): "On" state under forward bias in one single AVC cell

towards $n_{eff\_passive}$, and when the difference of them is small enough a strong optical coupling between the active and passive regions will happen. Under such circumstance, the lightwave transmitting in the passive region will be gradually coupled upwards into the active one, reflected by the corner mirror, and then coupled back down into the passive region again but now perpendicular to the original propagating direction. Thus in the topology of the $N \times N$ matrix with N input and output (I/O) ports, one specific route could be

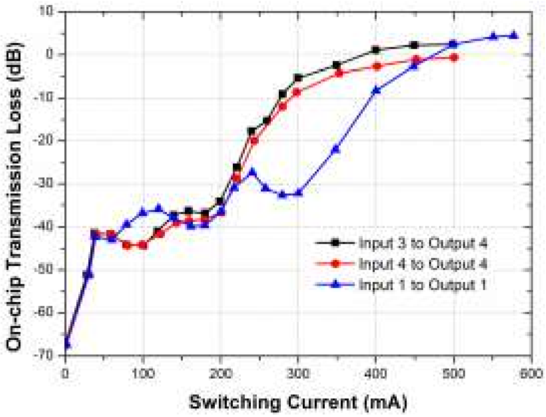

Fig. 3. The measured on-chip switching characteristic at 1550 nm in TE mode for separate AVC cells

selected and switched "On" by simply injecting the current into the AVC cell in the corresponding crosspoint of the switching matrix. An attractive feature of this architecture is that, irrespective of the size of the $N \times N$ switch matrix, only a single crosspoint is energized per input port, reducing drive complexity, power consumption and switching time compared with matrixes built up from 2 × 2 switch elements.

Fast switching performance was realized and the switching speed was previously measured to be smaller than 10 ns [10], adhering to the intrinsic characteristic of carrier injection. Besides, the active region also generates the optical gain when the injection exceeds the transparent carrier density, which is deliberately utilized to compensate for the signal transmission loss resulting from the fiber-chip coupling and on-chip transmission loss. As can be seen in Fig. 3, an on-chip transmission loss ~0 dB in TE mode under an injection current (I) of around 500 mA is noted via the measurement of both the longest (from Input port 4 to Output port 4) and the shortest route (from Input port 1 to Output port 1) on the OXS chip. The result of another arbitrarily-picked route is also included in the same figure and found to exhibit the similar IL performance, implying the uniformity among the switching cells. The measurement also shows under I = 0 mA, i.e. the "Off" state, an On-Off extinction ratio is higher than 65 dB, confirming an excellent crosstalk suppression.

III. Gen-2 4 × 4 Polarization-Independent CFP2 OXS Module

To better meet the requirements of the DCNs, a second generation (Gen-2) 4 × 4 OXS module which is based on the similar AVC-alike monolithic InP-based chip structures is proposed and under development currently. Polarization independent switching is one of the new features compared to the previous Gen-1. The switching characteristic test result as shown in Fig. 4(a) reveals that both the TE and TM mode exhibited almost the same switching transmission performance within the current range from 210 to 260 mA, indicating a polarization dependent loss (PDL) of <0.5 dB and the validity of the proposed PDL-control technology employed in the Gen-2 module. The observed relatively higher IL and lower On-Off extinction ratio in the primary Gen-2 sample devices are mainly due to the fab imperfections in the initial runs, and the higher fiber-chip coupling loss. These problems are expected to be solved in the following run with the optimized fab recipes and inclusion of the spot-size-converter (SSC).

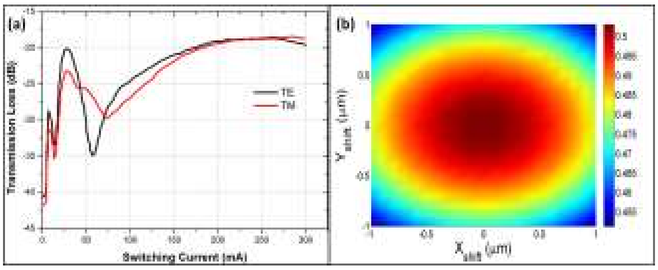

Fig. 4. (a): primary PDL switching test at 1550 nm for the AVC cell of Gen-2 OXS; and (b): The contour map of the calculated fiber-chip coupling efficiency with regard to the X and Y shift

Aiming for a robust and cost-efficient packaging, all the I/O ports of the OXS devices are re-arranged in parallel layout with an interval of 250 μm and positioned across the same cleaving facet of the chip, and a single-mode fiber-array ribbon with the same interval is butt-joint coupled to all the I/O ports in one alignment step. To reduce the coupling loss and achieve both high manufacturing yield and environmental stability, mode-expanding SSCs are further introduced into all the I/O ports in the latest fab run. According to the calculated result shown in Fig. 4(b), a coupling efficiency of 50% (3 dB) is achieved and its variation is observed to be less than 0.3 dB, even when the shift in *X/Y* direction is up to 1 μm for either TE or TM mode.

To give performance feedback to the driver control system, and provide long-term and over-temperature stability, integrated monitoring photodiodes (MPDs) are placed along the 4 fan-in and the other 4 fan-out light paths of the central 16 switching matrix. The inclusion of the MPDs here will help extract the real time on-chip powers in all the I/O ports, serving as a reference to dynamically optimize the specific driving condition for each of the 16 switching cells. The OXS chip is mounted onto a heat-sink carrier beneath which there is fitted a thermal electric cooler (TEC). A thermistor mounted on the OXS chip surface works with the TEC and driving control circuit to keep the OXS operating at a constant temperature.

Fig. 5 gives an image of the OXS packaging solution as a

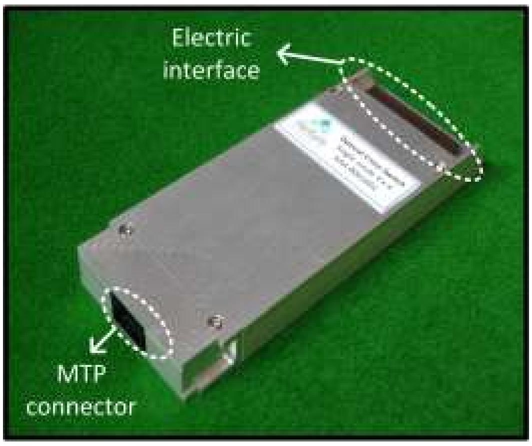

Fig. 5. The compact OXS module packaged in CFP2 form factor

CFP2 module. All the electrical connections are directed to the 104-pin connector in the rear side while all the optical connections converge into the MTP low loss fiber ribbon connector in the front side. The standard CFP2 pluggable module form provides easy installation and removal in the line-cards of the network equipment. It should be noted that with a module as small as CFP2, it will also be feasible to assemble several 4 × 4 OXS modules in parallel or cascaded configuration in the same line-card, to build up an even higher-port capacity such as 8 × 8 and 16 × 16 switching.

IV. CONCLUSION

In this paper we present the AVC-based Gen-1 and Gen-2 4 × 4 OXS module for FOS applications. The Gen-1 OXS module has shown a sub-10 ns lossless switching with an extremely low crosstalk level. Following the new PDL-suppressing approach, the Gen-2 OXS has demonstrated a polarization independent switching performance. Combined with a cost-effective packaging solution and the inclusion of other functional building blocks, the CFP2-typed Gen-2 OXS module is a promising candidate to serve as a FOS in future optical systems and networks.

ACKNOWLEDGMENT

This work is supported by European Commission Seventh Framework Programme (FP7/2001-2013) under grant agreement No. 619572, in the context of the COSIGN Project.

REFERENCES

[1] S. Yao, B. Mukherjee, and S. Dixit, "Advances in photonic packet switching: an overview," *IEEE Commun. Mag*., vol. 38, pp. 84-94, 2000.

[2] G. Zervas, R. Nejabati, Z. Wang, D. Simeonidou, S. Yu and M. O'Mahony, "A fully functional application-aware optical burst switched network test-bed," in *Proc. OFC 2007*, OWC2, 2007.

[3] A. Biberman and K. Bergman, "Optical interconnection networks for high-performance computing systems," *Rep. Prog. Phys*., vol. 75, pp. 1-15, 2012.

[4] C. Kachris, K. Kanonakis, and I. Tomkos, "Optical interconnection networks in data center: Recent trends and future challenges," *IEEE Commun. Mag*., vol. 51, pp. 39-45, 2013.

[5] R. Varrazza, I. B. Djordjevic and S. Yu, "Active vertical-coupler-based optical Crosspoint switch matrix for optical packet-switching applications," *IEEE J. Lightw. Technol*., vol. 22, pp. 2034-2042, 2004.

[6] S. Yu, S. Lee and R. Varrazza, "Lossless optical packet multicast using active vertical coupler based optical Crosspoint switch matrix," *IEEE J. Lightw. Technol*., vol. 23, pp. 2984-2992, 2005.

[7] S. Yan et. al., "Archon: A function programmable optical interconnect architecture for transparent intra and inter data center SDM/TDM/WDM networking," *IEEE J. Lightw. Technol*., vol. 33, pp. 1586-1595, 2015.

[8] K. Kant, "Power control of high speed network interconnects in data centers," *Workshop on High-speed Networks* (*HSN'09*), 2009.

[9] J. P. Weber, "Optimization of the carrier-induced effective index change in InGaAsP waveguides-application to tunable Bragg filters," *IEEE J. Quantum Electron*., vol. 30, pp. 1801-1816, 1994.

[10] N. Chi, J. J. V. Olmos, K. Thakulsukanant, Z. Wang, O. Ansell, S. Yu and D. Huang, "Experimental characteristics of optical crosspoint switch matrix and its applications in optical packet switching," *IEEE J. Lightw. Technol*., vol. 24, pp. 3646-3653, 2006.